Lawrence Berkeley National Laboratory
Energy Geosciences

Title
Flow of Gas and Liquid in Natural Media Containing Nanoporous Regions

Permalink
https://escholarship.org/uc/item/1fr695r0

Authors
Kneafsey, Timothy J
Borglin, Sharon

Publication Date
2019-09-06

DOI
10.1002/9781119066699.ch13

Peer reviewed

Flow of Gas and Liquid in Natural Media Containing Nanoporous Regions

Timothy J. Kneafsey, and Sharon Borglin
Lawrence Berkeley National Laboratory

Abstract

Flow in natural media with nanoporous regions is very complicated, with many governing processes. Well-developed numerical codes to integrate and model flow through these media are available. A great deal of very creative work has been done to understand individual processes governing flow in natural media with nanoporous regions, and both simple and elaborate tools have been used to gain process understanding. The complications in understanding and predicting flow in these rocks, particularly with multiscale heterogeneities, anisotropies, and the presence of multiple phases and large gradients are enormous. Here, we examine factors governing flow through natural porous media containing nanoporous regions. We present a conceptual model of the media, touch on the flow physics, and describe the techniques used to examine pore space in these rocks. In addition, we briefly describe some modeling of flow through these media. A number of processes which need better description are identified.
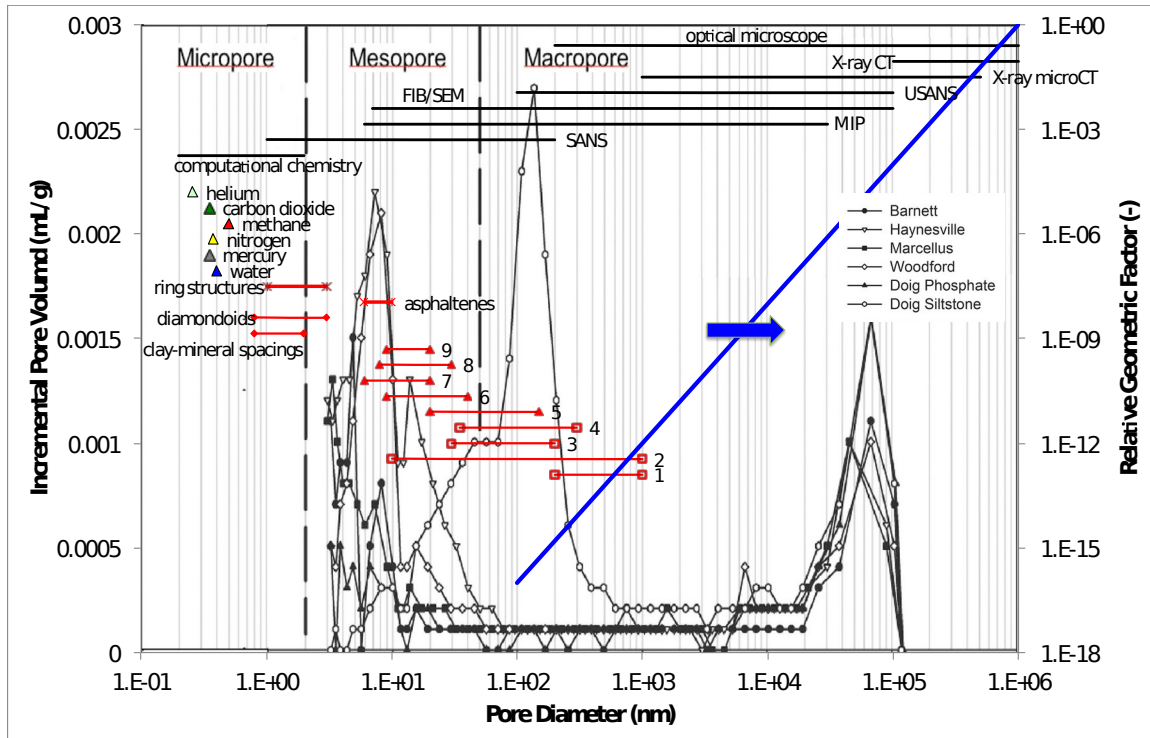
Introduction

The earth contains large regions with pores having dimensions less than 100 nm – herein called nanoporous media. Nanopores are different from larger pores because they are closer to the mean free path of molecules, or in some cases similar in size to molecules of interest, have a high surface area/ volume ratio, and are highly restrictive to flow. The presence of multiple phases in these pores will affect flow, because even adsorbed films will reduce the geometric area available for flow as well as altering wettability characteristics. In addition, capillary forces can be quite strong because of the small pore dimensions.

Understanding flow in these tight, low-permeability natural media containing nanoporous regions is important for a number of reasons. These include production of hydrocarbons (gas from shale and tight sandstone, light tight oil), geologic carbon dioxide sequestration (GCS), and minimizing flow and transport from waste repositories such as for nuclear waste disposal (WD). These media are present over large extents of the earth at various depths, and constitute perhaps 70% of sedimentary rock [*Britannica*, 2016]. Examples of natural porous media containing nanoporous regions include shales and chalks. Known shales associated with oil and gas production - representing only a portion of the global shales - are shown in Figure 1a.

The International Union of Pure and Applied Chemistry (IUPAC) has a classification system for pore sizes. IUPAC classifies macropores as pores with widths exceeding 50 nm, mesopores as pores with widths between 2 nm

and 50, and micropores as pores having widths not exceeding about 2 nm [*Sing*, 1985]. This terminology is a little confusing as each of these divisions includes nanometer-scale pores. Shales typically contain pores spanning these ranges, in addition to micron scale and even larger fractures (Figure 1b). Because we are considering natural media, which are inherently anisotropic and heterogeneous, we must consider multiple pore scales even in submillimeter-scale samples. Figure 1b illustrates this important point about natural porous media – pores range in size over multiple spatial scales. The black curves indicate the ranges of pore throat sizes measured in 6 shales by mercury injection porosimetry (described below) showing the presence of larger sub mm pores in addition to a range of macro- to micro-pores. Figure 1b also depicts the relative geometric coefficient for flow resistance related to the pore size. The blue line compares the flow resistance for pores of various sizes compared to that of a 1-mm pore. This will be discussed in more detail below.

Figure 1. Map of basins with assessed shale oil and shale gas formations, as of May 2013

Source: United States basins from U.S. Energy Information Administration and United States Geological Survey; other basins from ARI based on data from various published studies.

a.

b.

Figure 1. a. Map of assessed oil and gas shale basins. Source: U.S. Energy Information Administration, December 2015) http://www.eia.gov/analysis/studies/worldshalegas/images/fig1map_large.jpg
b. Black curves - Pore-size distribution for 6 shales defined by the pore volume from porosimetry analyses (from *Chalmers et al.*, 2012; see legend). For these shales, pore diameters range between 3 nm and 100 nm. The boundaries between micropores, mesopores, and macropores are highlighted by bold dashed lines. Red lines indicate the sizes of pore throats in four tight sandstones (1 - Upper Cretaceous Lance Fm., Greater Green River Basin, 2 - Upper Jurassic Bossier Interval, East Texas Basin, 3 - Upper Cretaceous Mesaverde Fm., 4 - Piceance Basin, Lower Cretaceous Travis Peak Fm.), five shales (5 - East Texas Basin, Pennsylvanian shales, 6 -Anadarko Basin, Pliocene shales, 7 - Beaufort-Mackenzie Basin, Source Rocks, various areas in the US, 8 - Devonian shales, Appalachian Basin, 9 - Jurassic-Cretaceous shales, Scotian shelf) and some molecules of interest (from *Nelson*, 2009). Measurement techniques are presented along the top (CT – computed tomography, USANS – ultra small angle neutron scattering, FIB/SEM – focused ion beam scanning electron microscopy, MIP – mercury injection porosimetry, SANS – small angle neutron scattering). Modified from Chalmers et al. (2012) and Nelson (2009) and used with permission. The blue line shows the relative geometric flow factor relative to the flow through a 1 mm pore. Note the range of values extends over 16 orders of magnitude.

Knowing the pore or pore throat size distribution is critically important for understanding flow in natural media containing nanoporous regions. But by itself knowledge of pore size distribution is insufficient to predict flow behavior. Other factors that can affect flow are porosity on multiple scales (sub-micron, micron, and larger) in organics, between grains, in pyrite framboids, fossils, within minerals and as microcracks. While the majority of pores in some shales are located in the organics, in other shales the porosity is largely associated with minerals [*Sondergeld et al.*, 2010]. Flow in nanoporous media is strongly affected by the pore size and geometric configuration of the pores, connectivity of the nanoscale pores to each other and to micron-scale and larger interconnected fractures and faults; fluids contained in the pores and their behavior under static and dynamic conditions; wettability distribution of the pore wall surfaces; the presence and properties of sorbed constituents on pore walls; overall anisotropy and heterogeneity of the mineral and organic fractions of the media; and the driving forces that induce flow.

As an example to set the background for the discussions in this chapter, for gas shales Javadpour et al. (2007) describes a number of processes that occur for gas to be released and transported through shale, including Darcy transport in micron-scale pores, Knudsen transport in nanopores, gas storage as compressed gas, adsorbed "gas" on solid kerogen and clays, and soluble "gas" in organic matter. In their study the permeability of 152 samples from 9 fields measured using pressure decay permeametry had a mode value of 54 nd, with 90% of the samples having a permeability less than 150 nd. Mercury injection analysis indicated that pores from 4 to 200 nm are dominant flow passages. Analyzing flow as a diffusive process with slip, they concluded that Knudsen diffusion can describe the flow. More on each of these topics is presented below.

In this chapter, pore-scale processes are discussed as a prelude to discussing aggregate or macroscopic-scale processes such as permeability and relative permeability, and larger-scale modeling where parameters are provided on the grid-block scale. The current chapter is organized as follows: first, a conceptual model is presented for the structure of tight natural nanoporous media and factors that influence flow. Secondly, a discussion of the physics describing flow and flow complications primarily at the pore-scale is presented, followed by a discussion of driving forces. Next, techniques used to understand the pore space are described, along with their advantages and disadvantages. Finally, flow measurement and modeling at the macroscopic (core and larger) scales is discussed.

Note that much of the literature cited in this chapter comes from petroleum industry conference papers (e.g. Society of Petroleum Engineers). Although many of these sources are not peer-reviewed, the observations, ideas, and content are very relevant and valid for understanding flow in natural porous

media containing nanoporous regions because this topic is of critical importance for the petroleum industry. With that in mind, observations and concepts are brought forward here.

General Conceptual Model of Natural Media Containing Nanoporous Regions

A general conceptual model of tight natural media from small to large scale is presented, as it pertains to flow in natural porous media containing nanoporous regions. This approach is most applicable to oil and gas production where extraction of fluids is desired, and in reverse for sequestration of fluids in GCS and WD applications. Compounds of interest (hydrocarbons, CO_2, radionuclides) may be present in very small pores in either fluid form (gas or liquid) or sorbed to the solid medium, which may be mineral or organic (e.g. kerogen). The locations of and phases present depend on the local thermodynamic conditions including chemical composition of the components in the pore, pressure, temperature, pore size, and pore wall surface chemistry.

Pores in the rock were formed during the lithification of the rock resulting from imperfect packing and compaction of the rock constituents (e.g. silts, clays, organic matter such as the remains of organisms) and incomplete secondary mineralization over very long time scales. Pores in the organic phases (kerogen) also formed over this time period, and additionally are influenced by the formation of oil and gas from original kerogen constituents resulting in pores up to micron or larger-scale, and perhaps their migration from the original formation location. Pores formed in the mineral media between grains are typically larger than the nanoscale micropores in kerogen, however some pores in kerogen can be quite large. Nanoscale pores, like all pores in porous media, may be of any shape and geometry [*Ambrose et al.*, 2010; *Chalmers et al.*, 2012; *Chi et al.*, 2015; *Curtis et al.*, 2011; *Desbois et al.*, 2009; *Dewers et al.*, 2012; *Elgmati et al.*, 2011; *Heath et al.*, 2012; *Heath et al.*, 2011; *King et al.*, 2015; *Loucks et al.*, 2009; *Silin and Kneafsey*, 2012; *Tomutsa et al.*, 2007; *Trebotich and Graves*, 2015]; may be contained in either mineral or organic fractions; and may be connected to networks of nanometer-to-micron scale pores.

Fluid flow in these media is governed by processes occurring over a range of scales. One important characteristic of nanopores is that they have a very high surface area to volume ratio influencing storage of sorbing compounds. In addition, sorbed molecules may become very restrictive to flow as they build up on the pore walls reducing the size of the flow paths. Another important factor is that pores sizes may be comparable to or smaller than the mean free path of gases present. The pores in mineral or organic networks may be connected to larger micro-scale pores or fractures, which in turn may be connected to larger fractures where flow occurs more rapidly. In shales, flow may be influenced by connection of nanoscale and microscale

pores through kerogen inclusions in the rock, which individually may contain significant porosity on the micron and larger scale.

The literature discussing observations of pores in shales focuses on the larger observable pores, often in kerogen inclusions. There is frequent mention of the interconnectedness of these inclusions and fluid-flow pathways between them. For example:

> Because pore networks in organic matter are most likely connected through microfractures, the connectivity of organic pore network can be significantly reduced in crushed samples.
> Organic matter is oil wet, and associated pores work as nanofilters of hydrocarbon flow and water blocking, suggesting that fluid flow in organic matter is predominantly single phase [*Wang and Reed*, 2009].

> Given that most pores are associated with organic matter, permeability pathways should be greatly influenced, if not controlled, by the three-dimensional arrangement of organic-matter grains. Connected organic matter could enable limited flow, depending on the connectivity of the nanopores within it. Preliminary observations suggest variations in the distribution of organic matter among samples that could account for variations in permeability [*Loucks et al.*, 2009].

Although such statements are common in the literature and perhaps not entirely unreasonable, most imaging studies have not been carried out on a scale or with the intention of identifying these interconnected paths, and the structure of these paths is inferred indirectly.

In addition to the complex pore connectedness and geometry, the surface chemistry of the pore walls is important, particularly when multiple phases are present. It is generally assumed and accepted that the mineral surfaces in shale are water-wetting, however, those in a kerogen inclusion may or may not be oil wetting [*Hu et al.*, 2014; *Odusina et al.*, 2011; *Wang and Reed*, 2009]. Distribution of the organic phases and maturation of the kerogen play a significant role in wettability, complicating multiphase flow understanding significantly [*Heath et al.*, 2012].

Flow Physics

Single-phase liquid fluid mechanics
Single-phase liquid flow in natural porous media containing nanoporous regions is important for light tight oil production, radionuclide transport from a nuclear waste repository, and disposal of brines. To gain an appreciation for flow physics "friendly" geometries and conditions will be examined first, although pores in natural tight rock may be of any geometry. For simple pore geometries such as a cylindrical pore or the space between two flat plates,

ignoring gravity, single-phase liquid laminar flow can be described by the Hagen-Poiseuille equation, shown below [*White*, 1979].

$$Q_{cylindrical\ pore} = \frac{\pi r^4 \Delta P}{8 \mu L} \text{ (1a)}$$

$$Q_{flat\ plate} = \frac{b h^3 \Delta P}{12 \mu L} \quad \text{(1b)}$$

In these equations, Q is volumetric flow rate, r is tube radius, h is the spacing between plates, b is the width of the slit, μ is viscosity, $\Delta P/L$ is the pressure gradient. If we assume that slit pore widths are in some way proportional to their aperture, this can be generalized to:

$$Q_{general} \quad \frac{d^n \Delta P}{\mu L} \text{ (1c)}$$

where d is a pore dimension and n is an exponent having a value of 4. The value in doing this is simply to show that as the pore size decreases for a given pressure gradient, the flow rate in pores decreases dramatically because of the large exponent. This is indicated by the blue line in Figure 1b - read on the right axis, showing only the magnitude of the geometric factor. This blue line compares the magnitude of the geometric factor with that for a 1 mm pore or slit. Note the right axis varies by 16 orders of magnitude over the range of pore sizes plotted. For example, a 1-micron diameter cylindrical pore is 10,000 times more conductive than a 100 nm diameter pore (Knudsen diffusion not included here). It is critical to understand the various contributions of different pore sizes to flow. Additionally, the length of the pore also plays an important role in flow resistance.

Single phase gas fluid mechanics
Where pressures are high and/or pores large, such that the molecular mean free path is small in comparison to the pore size, the physics described above applies to advective gas flow, however gas compressibility needs to be accounted for. Where pressures are low or pores very small such that the molecular mean free path is on the order of 100 times the pore size, the relative frequency of molecular collisions with the pore walls compared to those with the gas molecules themselves becomes very important, and results in slip at the gas-pore wall boundary. The Knudsen number is defined as $Kn = \frac{\acute{\lambda}}{r_{pore}}$, where $\acute{\lambda}$ is the mean free molecular path and r_{pore} is the equivalent hydraulic radius of the pore [*Freeman et al.*, 2011]. This number is used to distinguish gas flow regimes. Four regimes are typically considered [*Florence et al.*, 2007]. In the *Continuum Flow Regime*, $Kn < 0.01$, the mean free path of the gas molecules is much less than the hydraulic radius. Here, continuum fluid mechanics is applicable (*i.e.*, Navier-Stokes equations). In the *Slip-Flow Regime,* $0.01 < Kn < 0.1$, slip occurs in the "Knudsen" layer (layer of gas molecules immediately adjacent to the wall). The *Transition Regime* extends over the range $0.1 < Kn < 10$, and where $Kn > 10$ called the *Free Molecular Flow Regime*, the flow is dominated by diffusive effects.

Molecular dynamics and Lattice Boltzman simulations demonstrating slip flow are shown by Akkutlu and Fathi (2012) and Zhang et al. (2015).

Knudsen diffusion is often accounted for at the macroscopic scale in porous media using the Klinkenberg parameter to modify the permeability term [*Klinkenberg*, 1941].

$$k_a = k_0 \left(1 + \frac{b_K}{p} \right)$$

Here, k_a is the apparent permeability, k_0 is the intrinsic permeability, b_K is the Klinkenberg parameter, and p is pressure. A number of models providing a better fit of data have also been created [*Florence et al.*, 2007], but these also have the same general shape as the Klinkenberg model. Some values for b_K are listed in Wu et al. (1998) and methods to compute the apparent permeability are available [*Florence et al.*, 2007; *Freeman et al.*, 2011].

Realities of flow in natural nanoporous media
In most cases of interest in the natural environment, multiple fluid phases will be present in rock. These include formation brine, natural gas, oil, CO_2 in the case of GCS, and H_2 in the case of NWD. The presence of another fluid phase significantly reduces permeability [*Bennion and Bachu*, 2007; *Florence et al.*, 2007; *Jones and Owens*, 1980], particularly for nanoporous media.

With multiple phases, the interface and differences in pressure between fluid phases must be considered. The Young-Laplace equation describes the pressure difference across the curved interface between two fluids.

$$P_c = \gamma \left(\frac{1}{R_1} + \frac{1}{R_2} \right) cos\theta$$

In this equation, P_c is the pressure difference between the two phases, γ is the interfacial tension, R_1 and R_2 are perpendicular radii of curvature, and θ is the contact angle measured through the wetting phase normal to the contact line ($\theta = 0°$ for completely wetting, $\theta = 180°$ for completely nonwetting). For very small radii of curvature, the interfacial tension itself may change slightly [*Fisher and Israelachvili*, 1979; *Tolman*, 1949].

While conceptually simple, the contact angle, typically measured in the clean laboratory environment on polished flat surfaces with pure fluids, is strongly affected by soluble contaminants, especially amphiphilic compounds, as well as surface chemistry heterogeneities, and surface roughness. The contact line can become pinned at any surface imperfection and hinge at that location resulting in a phase becoming immobilized unless sufficient pressure builds up to move the pinned contact line. Additionally, even under ideal conditions, the advancing and receding contact angles are different.

An example of how this affects flow in nanoporous media is as follows. Consider an arbitrary shaped rough-walled pore with heterogeneous surface properties. A nonwetting phase (NWP – e.g. oil, gas, CO_2 for a hydrophilic

medium) will typically invade through the largest opening of the pore. If the pore widens in the flow direction or if the invading phase encounters a more NWP-wetting surface (higher contact angle through brine) invasion will be enhanced at constant capillary pressure. Conversely, higher capillary pressures are required to invade into a narrowing pore or encountering a more water-wetting surface. It is also possible that the contact line will pin at the wettability or surface feature change. Although it is conceptually easier to consider this in 2 dimensions, recall that the pores are three-dimensional, and typically part of a network, thus other pathways may be available for NWP invasion. When the phases completely block each other at the pore and aggregate scale, the condition is known as a permeability jail [*Blasingame*, 2008]. In formations where these conditions exist, imbibition of hydraulic fracturing water into the rock may cause a permeability jail to occur over some saturation conditions, hindering gas or oil flow through regions of the rock.

NWP flow in shale
Water is omnipresent in the subsurface environment as free phase liquid, sorbed to solid constituents such as mineral or even organic surfaces, and dissolved in other fluids. The presence of capillary bound water or even sorbed water will affect NWP flow through shale by reducing the available pore space for flow [*Sakhaee-Pour and Bryant*, 2012; *Wang and Reed*, 2009]. In gas shales, production of gas is strongly affected by the presence of water. Gas shales that produce well typically have less than 30% water saturation [*Wang and Reed*, 2009]. Such low initial water saturation may be caused by drying under paleo temperature and pressure conditions followed by cooling to current conditions [*Wang and Reed*, 2009], or by the formation and transport of gas from the shale evaporating water as it is mobilized.

Shale wettability
Because shales formed from subsea deposits, it is reasonable to consider most of the mineral surfaces to be hydrophilic. In shale, oil and gas formed from organic matter co-deposited with the mineral grains, and the oil or gas may have been subsequently transported over time through pathways through the shale. In so doing, these hydrocarbon fluids came into contact with pathways in the rock and could have affected their wettability [*Heath et al.*, 2012; *Wang and Reed*, 2009]. The wetting characteristics of the organic material remaining in the shale (kerogen) could be hydrophilic or hydrophobic depending on the chemical makeup and maturation [*Hu et al.*, 2014].

Ruppert et al. (2013) investigated two Mississippian Barnett Shale samples to identify the fraction of the pores accessible by deuterated methane (CD_4) and, separately, deuterated water (D_2O). In the two samples investigated, the total pore size distributions were essentially identical. For pores larger

than 250 nm, >85% of the pores in both samples were accessible to both CD_4 and D_2O. In the smaller pore sizes (~25 nm) in one sample, CD_4 penetrated the smallest pores as effectively as it did the larger ones. In the other sample, however, less than 70% of the smallest pores (<25 nm) were accessible to CD_4. These pores were still largely penetrable by water. It was noted that the composition of the material immediately surrounding the accessible (open) pores in the 25 nm size range was associated with either mineral matter or high reflectance organic material. These data indicate that for the samples and pore sizes analyzed, the medium was mainly water wetting.

Odusina et al. (2011) used NMR to investigate wetting behavior in Eagle Ford, Floyd, Barnett, and Woodford samples. Both brine and oil were imbibed in the shales. The volume of oil imbibed was influenced by a number of factors including a combination of shale Total Organic Carbon (TOC), thermal maturity, and organic pore volume. The authors assumed the organics present in the samples were oil wetting. Overall, the shales displayed mixed wettability. In addition, exposure to drilling fluids during sample collection could have affected the "as received" wettability state of the cores.

Tinni et al. (2015) used NMR to investigate wetting behavior of Haynesville, Barnett, and Woodford shales. They concluded that the brine-saturated porosity is always greater than the oil-saturated porosity implying that brine can enter the entire pore spectrum, but oil and methane have access only to the oil-wet-porosity fraction. Based on their measurements and the saturation processes used, a significant portion of the flow path is controlled by the fraction of pores that are water-wet.

NMR was also used by Gannaway (2014) to examine displacement of oil from shale by brine, through making measurements daily until no changes were observed. Water imbibition driving oil displacement indicated that there is a portion of the pore space that is water wetting. Gannaway devised a method that allowed computation of various types of porosity, including helium porosity (crushed), dodecane-saturated porosity, effective porosity, inorganic porosity, organic porosity, mixed porosity, and clay-bound water, quantifying wettability in bulk. This approach assesses temporal processes (flow, displacement) by making NMR measurements over time while different processes are occurring, for example imbibition, not simply providing a bulk measurement.

Sorption
In nano-scale pores, the presence and characteristics of the adsorbed layers of molecules on the mineral and organic surfaces will constrict flow and alter contact angles. Sakhaee-Pour and Bryant (2012) argue that the presence of adsorbed methane can reduce the geometric space available for flow to the

extent that laboratory measurements performed under poorly representative conditions may overestimate the permeability by a factor of up to 4. Hu and coworkers (2014) through molecular dynamics simulations examined the effect of the concentration of oxygenated compounds in the kerogen phase on the location and configuration of oil (octane) and water in the pore space. They show that for a pore in kerogen with added carbonyl groups, increasing the oxygen:carbon ratio to 1.6%, that water preferentially builds up in the pore reducing the geometric area available for oil to flow, whereas this does not happen for the less oxygenated kerogen model. They combine these geometric and chemical effects for a limited range of conditions, illustrating that diffusion of sorbed constituents also occurs along the surface of the pore, providing another mass transfer pathway. In shales this is poorly understood, generally assumed to be less important than other processes, and is typically ignored [*Freeman et al.*, 2011].

Multicomponent gases
In low permeability porous media, simply incorporating Fick's law into a convective flow equation does not adequately describe flow behavior [*Webb and Pruess*, 2003]. The Dusty Gas Model [*Thorstenson and Pollock*, 1989a] provides a more accurate description of behavior. Because the diffusivity of each component is dependent on its molecular mass, the transport rate of each component is different, and in a tight porous medium with small pores, some separation of the components may occur resulting in lighter components being more readily produced. Freeman et al. (2011) suggest that permeability estimates can be improved based on this separation, although very high quality gas chemistry measurements would be required.

Driving forces
Flow occurs in response to thermodynamic disequilibrium, thus can be caused by pressure, thermal, and chemical gradients. Flow resistance in media containing nanoporous regions is very high, owing to factors already mentioned. The major driving forces typically of concern are anthropogenic pressure changes. When producing fluids, low pressures are induced in wells and connected fractures. When introducing fluids, elevated pressure occurs in the well and connected fractures. The low permeability, chemical interactions, and temperature differences adjacent to fractures or wells result in steep gradients resulting in large fluid property changes (e.g. viscosity, density) over short distances making fluid transport modeling difficult.

Osmotic effects are induced by the difference in the water activity in the shale and the water activity in the introduced fluids such as drilling mud or hydraulic fracturing fluids. The water activity is strongly impacted by the type and concentration of dissolved species in the water. The semi-permeable membrane between the two fluids is the shale medium and the mudcake (if present) at the borehole or fracture wall. Very high salinities (up

to 300 g/L [*Arthur and Cole*, 2014]) have been observed indicating that osmotic effects can be high if the injected water is dilute. In laboratory experiments, imbibition of water due to osmotic effects was responsible for enhancing production of oil from Bakken cores [*Fakcharoenphol et al.*, 2014]. In gas shales, where salinity can also be very high and brine saturation low, osmosis may also enhance fracturing fluid uptake resulting in phase trapping [*Bennion*, 2002].

Ignoring geologic timescales, pressure, temperature, and chemistry have the strongest influence on flow. Pressure, temperature, and chemistry effects near the wellbore and connected fractures strongly alter how we perceive reservoir behavior. For example, thermal diffusion into formations from the wellbore induces additional pore pressure and rock stress changes, in turn affecting wellbore stability. Thermal diffusion into shale may occur faster than hydraulic diffusion providing the dominant effect at early times [*Chen et al.*, 2003]. The effects and responses to thermal gradients can be large in some natural media, however these media typically have moderate permeability in relation to the time and spatial scale of the perturbation. For most tight natural media, thermal gradients will not significantly affect flow. Chemistry can affect the medium behavior, particularly if swelling clays are present and the injected fluid is more dilute than the local brine resulting in swelling, affecting both permeability and mechanical properties of the medium.

Methods of Examination
Because the pore space is where the fluids flow, understanding pore space structure is very important. However, understanding the kinetic component is necessary to understand flow. A number of methods have been used to investigate the structure of tight porous medium providing valuable but partial information. If each technique is used alone, results can be biased and not provide a complete understanding of pore structure. The majority of the techniques examine the pore space, fewer are useful in examining flow. Pore space examination techniques will be discussed, along with the advantages and disadvantages of each method. Macroscopic-scale methods will be discussed as well. Prior to discussing the techniques, however, it is important to discuss the artifacts caused by sampling.

Sampling
Before a sample can be tested by any technique, it must be collected, handled, examined, and brought to the measurement device. All samples suffer from several biases. First, even if they could be perfectly collected, they are small relative to the region they are assigned to represent. For example, a standard core sample (3.8 cm diameter x 10 cm length) with a volume of 114 cm^3 is on the order of 10^{-12} of a fracture stage volume, whereas a typical focused ion beam-scanning electron microscopy (FIB-SEM) volume is on the order of 10^{-22} of a fracture stage volume ($\sim 30 \times 10^6$ m^3)

[*Cipolla et al.*, 2008; *Cipolla et al.*, 2010]. Although measurements on these scales are very informative, it is unlikely that values extracted for a FIB-SEM volume would be assigned to a reservoir for modeling purposes nor should they be. Collection and selection processes are fraught with the inherent bias of the collector or the needs for a particular test. For example, if a 5 cm diameter x 10 cm length core is required, only certain pieces of retrieved rock can be used and in specific orientations. It is crucial to understand whether these pieces of rock are truly representative. To test a sample, it must be removed from its natural stresses (unloaded) when sampled, and then often transferred to a collection container that might not preserve the water activity (function of temperature, relative humidity, salinity) or other conditions.

Outcrop Samples
Relevant samples are available in the deep subsurface and must be collected from there. Outcrop samples, while easier to obtain, have been exposed to much different conditions, including much lower lithostatic stress and different redox conditions. Study of such samples is *not* useless however, but investigators face the difficult task of trying to understand the differences between their samples and the properties of the formation of interest.

Reservoir Samples
Reservoir core samples from the deep subsurface are much more difficult to obtain than outcrop samples and are very valuable. They are subject to contradictory needs, such as the need to preserve a record of the medium at depth, and the need to destructively subsample and test the recovered samples. Because of the difficulty in collecting them, they might also be held back for a later possible future study, and not fully interrogated following collection. All samples retrieved from depth are compromised to some degree. These samples have had their stress unloaded changing their geomechanical and hydrologic properties, and may be covered in drilling mud, which may alter the samples natural geochemistry. Collection of samples under native pore pressure is possible, however this is an expensive and difficult process, leading to core handling and testing difficulties. As with outcrop samples, investigators must be willing to understand the differences between their samples and the rock in-situ.

In-situ Tests
In-situ tests (in this chapter meaning "in its original place", not to be confused with tests performed under reimposed native conditions), in which rock in place is tested, do not suffer from all the problems of core samples and outcrop samples. Changes in the rock do occur from stress changes due to the removal of the core material, severe vibration and nearby rock failure from the drilling process, and drilling fluids, which have a different chemistry than the native fluids. Tests that can be performed in-situ suffer less from representativeness, because they are typically examining a larger region of

rock than core samples. They do suffer in that most of the measurements made are less-direct and often have larger error bars than laboratory measurements.

Whether outcrop, core, pressure core, or in-situ, the best direct observation techniques that can be applied should be applied. These include visual observation, photography, microscopic examination of samples and thin sections. These observations need to be made as soon as possible for core samples and again when they are tested. Other important techniques are discussed below.

X-ray Computed Tomography (CT)
Beyond direct visual and optical examination, X-ray computed tomography (CT) at available scales can also be performed to understand the material structure at these scales. Scanning can be performed at the core scale providing general information of the medium structure. Advantages of this method include simplicity, the ability to examine the sample through the packaging, the ability to select subsamples based on test criteria, and the method is nondestructive. Disadvantages include the availability of equipment, and imperfection in interpretation of the results. Scanning is typically performed in a laboratory (sometimes a hospital), although field transportable X-ray CT scanners have been constructed and used [*Freifeld et al.*, 2006]. In the lab, natural conditions can sometimes be reimposed on samples for better understanding. This requires using light element coreholders (carbon fiber, PEEK, beryllium, aluminum, titanium) that are X-ray "transparent". None of these are completely X-ray transparent, and all cause some degree of image degradation due to X-ray filtering.

When interpreting CT results, it is important to understand that the data portray the X-ray density at the energies applied for the voxel size selected with measurement noise. For heterogeneous materials, the apparent density of a voxel is composed of all the matter in the voxel. Two voxels having the same apparent density can be composed of entirely different materials, for example one composed entirely of medium-density matter, the other partly empty and partly filled with high-density matter. Flow through the second will likely be more important than the first. Thus, it is important to examine data relative to the entire data set. Many artifacts can occur on reconstruction of CT data, and techniques have been developed to mitigate their effects.

CT has been used to identify gas flow pathways in shales and coals [*Vega et al.*, 2014; *Watson and Mudra*, 1994]. By comparing CT scans of fully evacuated and xenon or krypton invaded samples over time, the invasion process has been observed, and the porosity map of the gas-filled sample can be determined. This is very important as flow can be tracked in real time over the spatial extent to which it occurs.

Figure 2 a-c shows three X-ray CT cross sections of a 12 cm diameter Opalinus clay core sample, Figure 2d shows a 3-D view of the high-density inclusions through the core - seen as white spots in the cross sections. Many of these are perpendicular to the bedding planes clearly identified by low-density (dark) features. Understanding flow through a region composed of these materials requires understanding:

1. the representativeness of the sample to the modeled region (how is the sample different from its native environment?)
2. flow in the higher-density layers, and flow in the lower density interbed layers (Note that in Figure 2a-d, the apparent "fractures" are indeed still rock and have an indicated density near 1.9 g/cm^3.)
3. flow in and near the high-density pathways that are oriented other-than-parallel to the bedding
4. the relative frequency of sizes and types of flow pathways relative to the directions of interest
5. whether the angled left boundary of the sample (in Figure 2b) is the face of a natural fracture through the clay which could be a major fluid flow path, or what is the distance to such a flow path

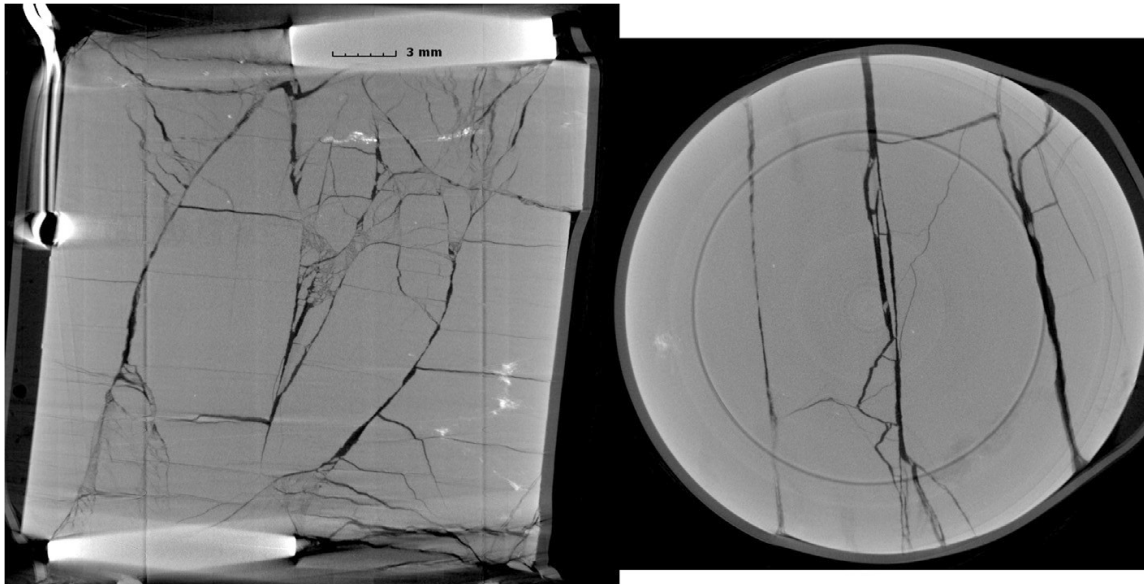a.   b.
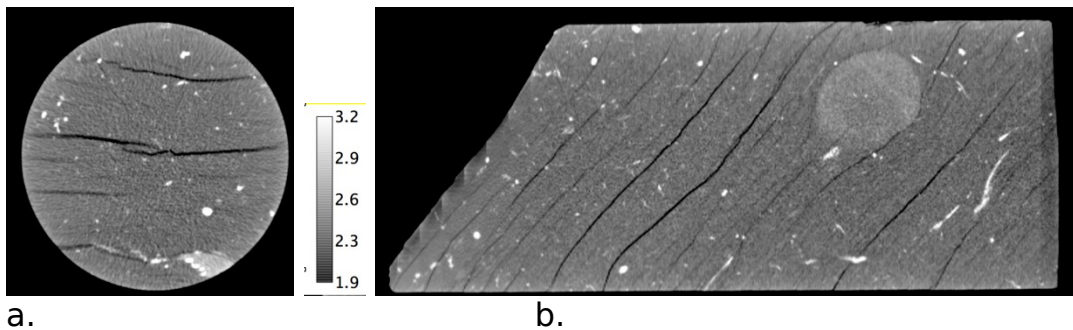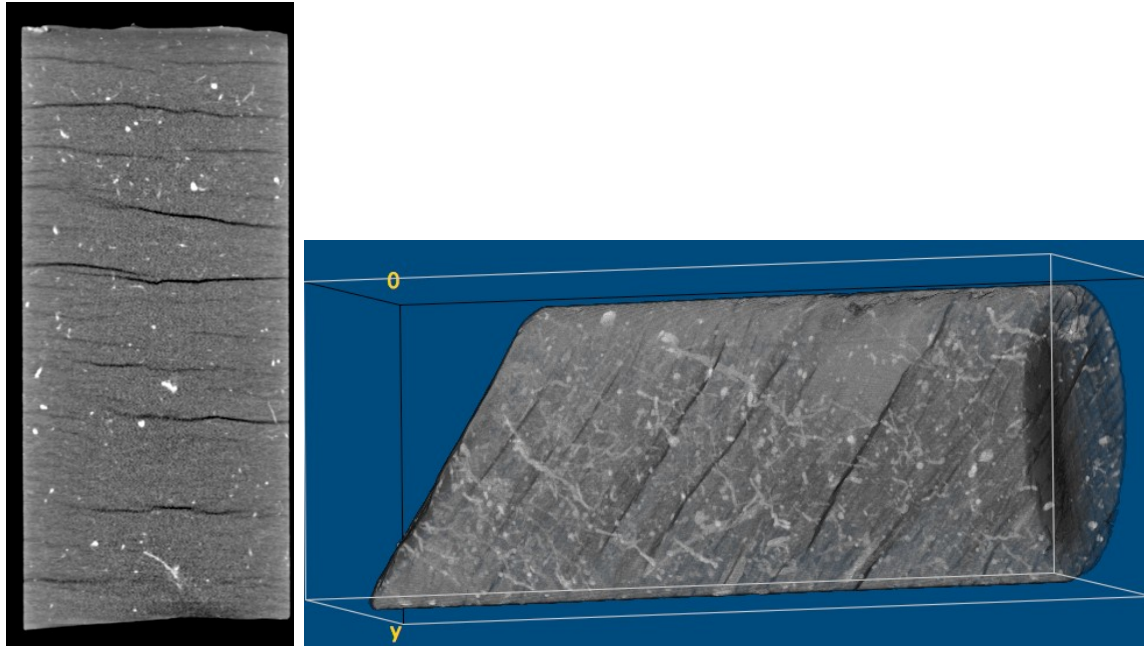
c.

d.

e.

Figure 2. a, b, and c. Cross sections of X-ray CT scans of a 12 cm diameter Opalinus clay core using a medical CT scanner with approximate density shown on the greyscale bar. Voxel size is 253 x 253 x 625 microns. ImageJ [*Rasband*, 2015] was used for data presentation. A beam-hardening artifact diminishes the appearance of the low-density features at the outer radii of the image. d. 3-D view showing the low-density bedding layers in dark and the high-density inclusions in lightest gray. (Volume Viewer Plugin for ImageJ by Kai Uwe Barthel). e. high-resolution X-ray CT scan of a fractured Utica shale sample (25 micron resolution) from *Carey et al.*, (2015), Reprinted from Carey, J. W., Z. Lei, E. Rougier, H. Mori, and H. Viswanathan (2015), Fracture-permeability behavior of shale, *Journal of Unconventional Oil and*

16

Figure 2e. shows a high-resolution X-ray CT cross section of Utica shale subjected to mechanical stresses inducing fracturing. This image provides detailed information on how fracturing occurs in the shale, providing an idea of flow paths generated and distances to these flow paths from interior regions of the shale.

High-resolution X-ray CT, microCT, and nanoCT
High resolution CT and microCT can be used to better understand rock structure at the ~micron scale and provide insights into pore structure. Most individual shale pores cannot be imaged at this scale, however the nature and structure of microfractures can be investigated among other things. The advantages of high-resolution CT and microCT are that they show the material structure at a much smaller scale (tens of microns for high resolution CT, ~micron-scale for microCT), and can be performed under reimposed natural conditions. As with coarser scale imaging, reimposing natural conditions requires the use of a core holder, and this will reduce the image quality. Disadvantages of this method are that only a small volume can be imaged. For microCT, samples are small and scanned volumes are typically less than 300 cubic mm depending on the time available and the scanning resolution desired. Samples must be machined for use, generally involving the use of a cutting fluid which may alter the sample. Even higher resolution nanoCT systems are commercially available, with voxel sizes as small as 50 nm on a side. Preparing a sample often requires laser ablation to machine the sample down to a reasonable size, typically on the order of 1000 times the voxel size.

Figure 3 shows cross sections of samples of Barnett shale and Marcellus shale, as well as segmented micro-cracks extracted from 3-D images of Mancos and a New Albany shale microCT data. Cracks having different shapes cut through the samples and vary in nature and frequency. Because of the image resolution, the interconnectedness of the fractures, particularly in Figure 2d is not known. Smaller flow pathways may be present at spatial scales beneath the resolution attained. In spite of these samples being several orders of magnitude smaller than the sample in Figure 2, similarities are apparent including identifiable bedding planes and noticeable anisotropy and heterogeneity. It is not known whether the larger cracks were present in the sample prior to sample collection. It is likely, however, that these cracks existed as weak zones even if they were not open in the subsurface. These images help in supporting a conceptual model of flow through some length of nanopores in the matrix to microfractures, which may be part of a larger network of fractures (Figure 3c), or dead-end fractures like in (Figure 3d).

It is important to note that all of these samples were imaged without stresses applied. In addition, the samples were machined into ~ 5 mm cylinders prior to imaging. The machining used either water or gas as the cutting fluid, and either might affect the sample, particularly if swelling clays are present. Imaging was performed under air-dry conditions, and this drying may also change the sample by removing or adding moisture and providing oxygen that may react with minerals in the rock.
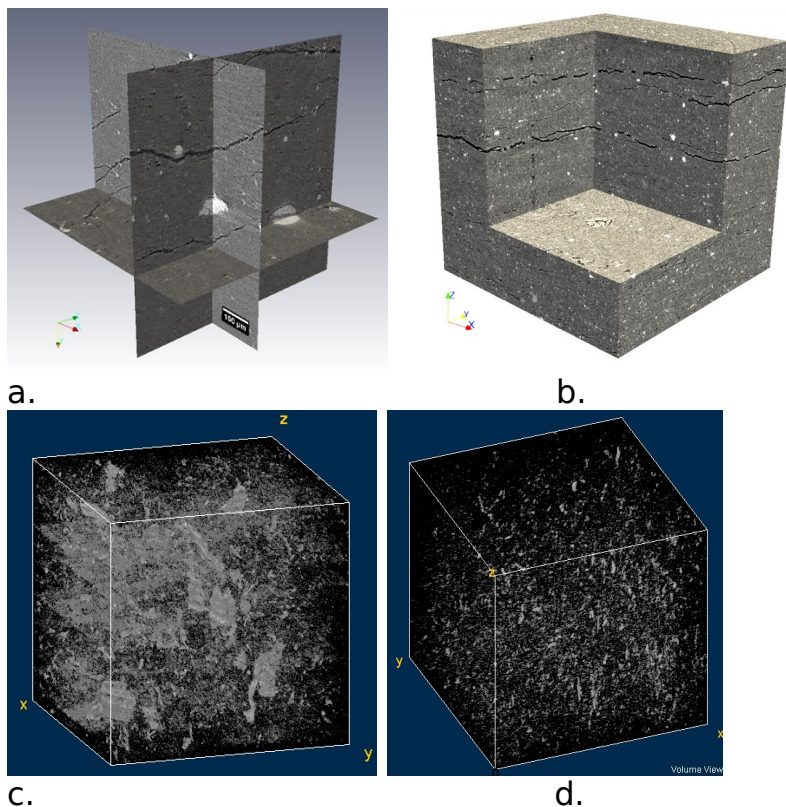

a.   b.

c.   d.

Figure 3. MicroCT orthoview of a. Barnett shale (scale bar = 100 microns), b. Marcellus shale (block side = 1.3 mm) and segmented microcracks in c. Mancos and d. New Albany Shale. (Ajo-Franklin and Silin, unpublished)

Focused Ion Beam-Scanning Electron Microscopy (FIB-SEM)
Focused Ion Beam-Scanning Electron Microscopy (FIB-SEM) is a technique where a focused ion beam is used to mill a nearly flat surface in a material, and the surface is then imaged using scanning electron microscopy (Tomutsa et al. 2007, Desbois et al. 2009, Loucks et al. 2009, Ambrose et al. 2010, Curtis et al. 2011, Elgmati et al. 2011, Heath et al. 2011, Chalmers et al. 2012, Dewers et al. 2012, Heath et al. 2012, Silin and Kneafsey 2012, Chi et al. 2015, King et al. 2015, Trebotich and Graves 2015). It is important to consider when viewing numbers of similar images that the observed pores have typically been sectioned at a somewhat random angle, thus are likely to have a similar aspect ratio in the dimension into the page as well (circular pores are more likely spherical than cylindrical). Sequential milling of thin

layers and imaging can be performed to extract the 3-D structure with voxel sizes ranging down to less than 10 nm [*Chalmers et al.*, 2012; *Dewers et al.*, 2012]. Few fully 3-D images are available in the literature. Computational fluid dynamics modeling can be performed to aid in understanding flow through the pores [*Dewers et al.*, 2012; *Trebotich and Graves*, 2015] although these techniques can be computationally expensive.

Prior to imaging, the sample is machined to fit on an SEM stub, and coated with a conductive material such as gold or platinum. Because the entire process is performed under a high vacuum, the sample is very dry affecting swelling clays. Typical volumes investigated using this method are on the order of 15 microns on a side depending on instrument time available and resolution desired, with higher resolution requiring more milling time at low current and longer imaging times. At 50 nm voxel size, volumes as high as 100 microns on a side have been imaged using argon plasma to mill (Figure 4a). Method limitations include grain size, image size, lack of confining stress, and upscaling [*Chalmers et al.*, 2012; *Slatt and O'Brien*, 2014]. A difficulty with FIB-SEM is selecting the site for imaging resulting in a sampling bias. The subsurface features are not clear from the top view of the shale. Many FIB-SEM studies of shales and chalks [*Yoon and Dewers*, 2013] have investigated interesting regions of study (Figure 4b), however, sometimes investigations that do not find interesting regions (Figure 4c) are rarely presented although conceptual models should include these features as well. Another limitation of the FIB-SEM technique is that larger features and rare features may not be observed at all [*Sigal*, 2015].

Imaging the location where fluids would be present can be performed using cryo-techniques combined with FIB-SEM [*Desbois et al.*, 2009], in which the sample is maintained at a very low temperature. The fluids are solidified in the process, but are subject to sublimation under vacuum while imaging. This method is subject to sample changes upon freezing from differential volumetric changes of the phases in the sample as well as the other limitations of the FIB-SEM technique.

Scanning Transmission Electron Microscopy
Heath et al (2012) used Scanning Transmission Electron Microscopy (STEM) in combination with FIB-SEM to examine pore-lining materials from the perspective of CO_2 wetting for GCS. These authors noted that pore-lining minerals are not always reflective of bulk mineralogy and also noted the presence of organic pore-lining materials in some pores. It was not possible to identify the wettability of the organic material. Based on partial CO_2 wettability to coal, they considered the possibility that all pores may not be water-wetting in the CO_2-brine-rock system
[*Heath et al.*, 2012]. The sample size used in STEM is even smaller than those imaged using FIB-SEM and those imaged by Heath (2012) are on the order of 100 nm thick, milled using a FIB (Figure 4d).

Helium Ion Microscopy
Multibeam scanning helium ion microscopes have demonstrated sub-nanometer resolution (Figure 4e). Few studies have been performed investigating the nanoporosity in natural porous media. Studies performed have shown pores and structures in amazing detail, and further study will lead to improvements in conceptual models [*King et al.*, 2015].

a.

b.

c.

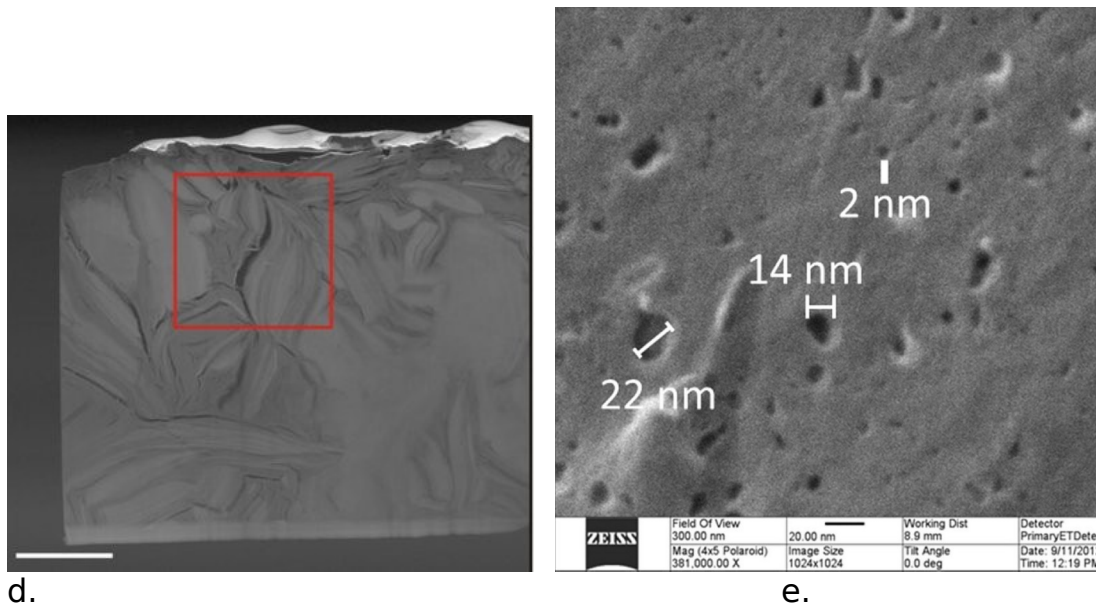d.   e.
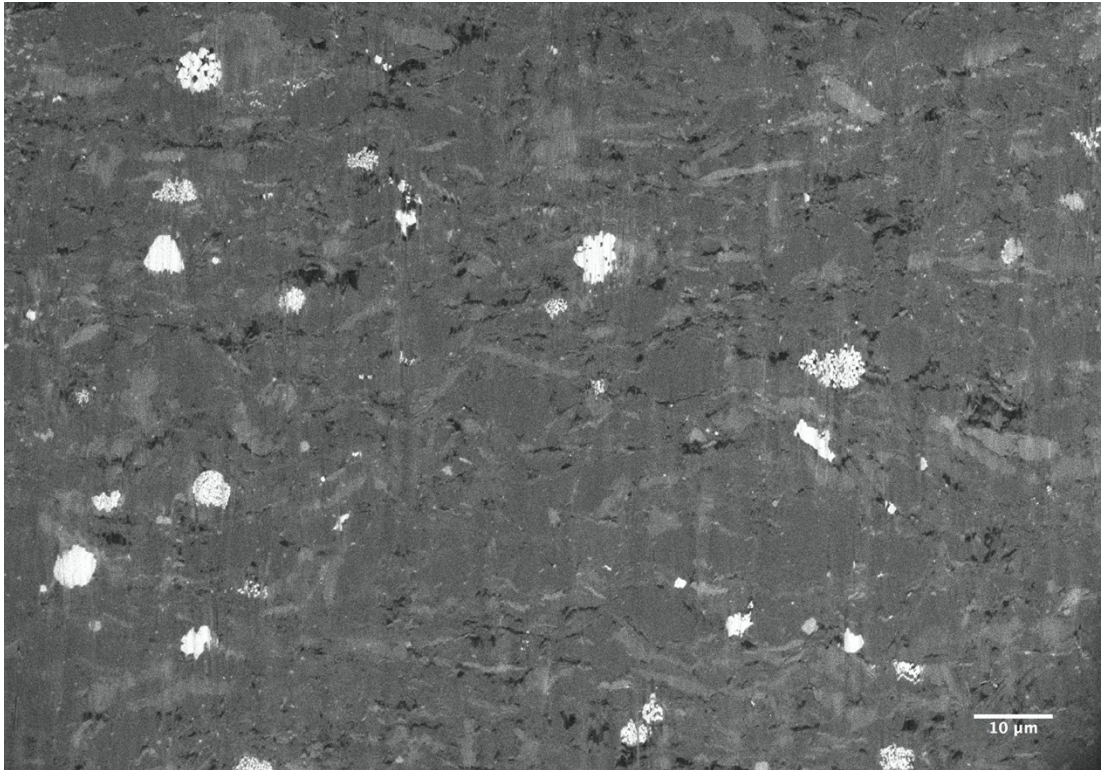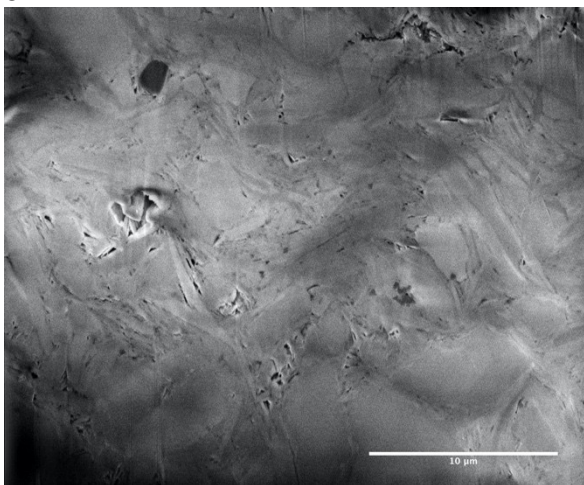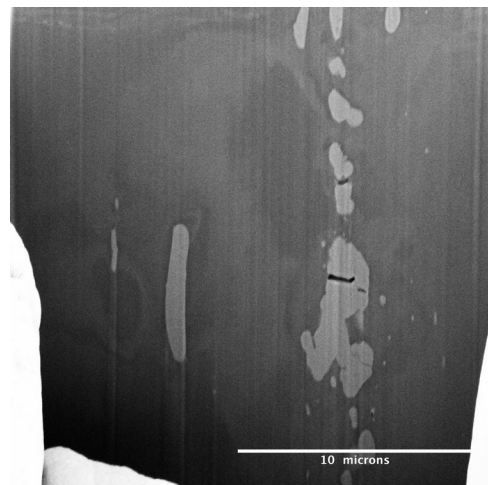
Figure 4. a-c. SEM images of FIB-milled Marcellus shale. a One of 1,330 50 nm slices showing
140-micron x 100-micron field of view d. High-angle annular dark-field STEM image of
Kirtland shale 820 m depth. Red box delineates region of additional analysis (from *Heath et
al.*, 2012, "Reprinted from Heath, J. E., T. A. Dewers, B. J. O. L. McPherson, M. B.
Nemer, and P. G. Kotula (2012), Pore-lining phases and capillary breakthrough pressure of
mudstone caprocks: Sealing efficiency of geologic CO2 storage sites, *International Journal
of Greenhouse Gas Control*, *11*, 204-220, doi:10.1016/j.ijggc.2012.08.001, with
permission from Elsevier.), e. Helium ion microscopy images of Evie shale showing
abundant porosity in organic matter with a wide range in the size of meso-
and micropores (from *King et al.*, 2015, Reprinted with permission from
King, H. E., A. P. R. Eberle, C. C. Walters, C. E. Kliewer, D. Ertas, and C.
Huynh (2015), Pore Architecture and Connectivity in Gas Shale, *Energy &
Fuels*, *29*(3), 1375-1390, doi:10.1021/ef502402e. Copyright 2015
American Chemical Society.). Figure 4a was imaged by Lisa Chan at
Tescan.

Mercury Injection Capillary Pressure Porosimetry (MICP)
Injecting high surface tension mercury into rock at sequentially higher
pressures allows quantification of porosity and pore throat distribution. This
method is commonly used in petrophysics laboratories. A large quantity of
data have been collected for a very large number of samples related to oil
and gas exploration [*Heath et al.*, 2012]. In MICP, nonwetting mercury is
forced into the evacuated pores of a crushed and dried rock sample, and
based on the surface tension of mercury and an assumed contact angle, the
volume of mercury injected and the injection pressure are used to compute
pore *throat* sizes. Pressures of up to 60,000 psi or more may be used to
quantify pores down to 2 nm. To force the injection to occur parallel or
perpendicular to the bedding, small samples can be epoxy-coated. Uncoated
samples can be used for omnidirectional intrusion. MICP investigates

connected pore space and ignores isolated pore space, which is appropriate for understanding where fluids may flow. Method limitations include sample crushing and dehydration which potentially alter pore sizes [*Bustin et al.*, 2008], and the method is sensitive to pore throat sizes [*Clarkson et al.*, 2013]. Bustin et al. (2008) suggest combining mercury porosimetry data with low-pressure carbon dioxide and nitrogen adsorption analyses (see below) provide a comprehensive pore size distribution analysis. Agreement of the methods should not be expected, however, because different analytical methods, based on different assumptions and theories are used for the computations.

Small angle neutron scattering (SANS) and Ultrasmall angle neutron scattering (USANS)
Unlike MICP, small angle neutron scattering (SANS) and ultrasmall angle neutron scattering (USANS) measurements record the scattering from all pores in a material, including pores that are inaccessible to fluids [*Ruppert et al.*, 2013]. USANS is used to investigate scattering at very small angles to study larger pores (10 µm to 100 nm), whereas SANS investigates larger scattering angles to study smaller pores (<250 nm). Clarkson at al. (2013) suggest adding SANS/USANS to the combination of tools suggested by Bustin et al. (2008) (low-pressure adsorption and high-pressure mercury injection) to be an effective approach for fully characterizing the pore structure of shales.

Nuclear Magnetic Resonance (NMR)
NMR has been long used to study pores in porous media, their availability to different phases, and wettability effects [*Anderson*, 1986; *Brown and Fatt*, 1956]. Anderson (1986) provides a very direct explanation of the processes. During NMR, protons align under a high magnetic field. When that field is replaced by a lower magnetic field, the alignment of the protons relaxes over time and this relaxation time is measured. If a proton is located near a pore surface, the relaxation time is impacted by the surface, and this can be used to infer wettability.

Sigal (2015) used an NMR technique to describe the pore space in small core samples under 5000 psi confining pressure and 4000 psi pore pressure. In the three samples investigated, the pore size distributions ranged from 0.2 nm to ~200 nm with modes of 18, 51, and 54 nm with 20 to 40% of the pore volume being contained in pores that are less than 10 nm in diameter where deviation from bulk-fluid behavior can be significant. When NMR was applied to dry-gas reservoir samples, pore sizes ranging from 1 to ~ 100 nm contained methane.

Sorption capacity
Low-pressure carbon dioxide equilibrium isotherms collected at 0°C (ice/water bath) can be used for determination of micropore capacities,

enabled by the Dubinin-Radushkevich (D-R) equation [*Dubinin*, 1989]. Nitrogen sorption at -196°C with the Brunauer, Emmett, and Teller (BET) equation [*Brunauer et al.*, 1938] can be used to quantify macropores to larger micropores from nitrogen sorption data [*Bustin et al.*, 2008]. For cumulative and differential volume distributions in the mesopore range, Barrett, Joyner, Halenda (BJH) theory [*Barrett et al.*, 1951] can be used from the desorption branch of the nitrogen isotherm. An important limitation of these sorption analyses is that they require the samples to be dry since a high vacuum is required for the analyses, thus the impact of drying shales on the pore structure is shale specific and must be considered particularly for poorly indurated, moisture, and clay-rich shales.

Permeability
The best indication of flow in tight media is the rock permeability, which does not rely on any description of the pore network structure. Permeability describes the ability of the material to transmit fluid under a set of conditions, which can be controlled in the laboratory to a certain extent. Permeability describes the ensemble of flow through the *flowable, connected* pore space of the medium at the scale of the measurement, including changes in connected and flowable pathways by sample preparation. It does not describe flow into or out of anastomosing dead-end pores, which is also critically important in the behavior of natural tight media. Analysis of pressure decay permeametry data can provide this value however.

In the laboratory, tight rock permeability is typically measured using a transient method, such as a pressure decay method. In the method, a pressure "pulse" is applied to the sample, and the pressure decay is measured as the gas flows into or through the sample and this is related to the permeability. Samples can be jacketed cores, in which both the upstream and downstream pressures are monitored over time, or crushed samples where the overall pressure decay is monitored. Measurements at different pressures can be inverted to estimate the Klinkenberg parameter [*Wu et al.*, 1998]. Measurements can be made for either intact or crushed rock samples, with the time needed to measure permeability increasing with the square of the sample size [*Carles et al.*, 2007], thus significantly shorter for crushed samples because of the high surface area and the small distance to the center of the grains. Because of this, most commercial measurements are made using a pressure pulse decay method on crushed rock. Permeability values measured in core plugs are significantly higher than those using crushed samples [*Wang and Reed*, 2009] perhaps because the core plugs contain permeability along the weakness boundaries in which the rock breaks upon crushing.

In a study of 22 tight sandstone samples, permeability was reduced significantly by the application of confining pressure [*Jones and Owens*, 1980]. The permeability of shales varies by several orders of magnitude with

effective stress. The degree of permeability reduction with increasing confining pressure is significantly higher in shale compared to consolidated sandstone or carbonate. Therefore representative shale-gas permeability measurements must be made at a confining stresses close to lithostatic stress at reservoir depth [*Wang and Reed*, 2009]. The presence of water also severely reduces gas permeability measurements, with the effect being stronger for lower permeability samples. Measurement techniques that do not consider effective stress including crushed rock permeability, permeability estimated from mercury injection porosimetry and from desorption data are instructional, but may be of limited direct use [*Bustin et al.*, 2008].

Few measurements of relative permeability in shales have been published. This is probably because the tests are difficult to set up and run because the low permeability inhibits establishing appropriate initial conditions, and extreme care is often needed for extended time to make the measurements. In making a comprehensive set of measurements on a series of samples including shales targeted at CO2/brine behavior, [*Bachu and Bennion*, 2008; *Bennion and Bachu*, 2005, 2007, 2008], it was noticed that all samples induced some brine displacement and CO_2 invasion under high pressure, however the CO_2 relative permeabilities were in the 10^{-12} to 10^{-10} darcy range. Similar to the observations of Jones and Owens (1980) who noticed that the presence of small quantities of water significantly reduced permeability for tight sands, Bennion and Bachu noticed that the presence of even a minor amount of the trapped CO_2 had a significant effect on the brine permeability. They noticed that there was not a clear correlation between porosity and pore size distribution and the initial brine permeability and relative permeability properties of the samples they evaluated. Finally, in comparison to reservoir quality rock, they noted that the shale permeability to brine was much lower, the efficiency of displacement of brine by CO_2 was much lower resulting in high saturations of trapped water, and that CO_2 trapped in the matrix resulted in extreme relative permeability hysteresis.

Modeling
Outside of the computational fluid dynamics studies briefly mentioned for pore-scale modeling, a number of models are available to describe flow in tight porous media. Although many models have been formulated for macroscopic scale simulation including scientific codes and reservoir simulators (for example: [*Akkutlu and Fathi*, 2012; *Alnoaimi et al.*, 2015; *Cipolla et al.*, 2010; *Civan*, 2013; *Freeman et al.*, 2011; *Meakin and Tartakovsky*, 2009; *Mehmani et al.*, 2013; *Montiero et al.*, 2013; *Moridis and Freeman*, 2014; *Nobakht and Clarkson*, 2011; *Ozkan et al.*, 2010; *Silin and Kneafsey*, 2012; *Umeda et al.*, 2014; *Wu*, 2015; *Wu et al.*, 1998]), only a few will be briefly discussed here. Conventional approaches include incorporating impacts of tight medium flow into traditional reservoir simulators [*Cipolla et al.*, 2010; *Moridis and Freeman*, 2014; *Wu*, 2015; *Wu et al.*, 1998]. Others

start with a different conceptual model and approach, for example [*Montiero et al.*, 2013; *Silin and Kneafsey*, 2012].

Powerful commercial simulators with specialized options for unconventional reservoir analysis are available including GEM [*Computer Modelling Group*, 2016] and ECLIPSE For Unconventionals [*Schlumberger*, 2016]. These reservoir-scale production evaluation codes address the most common features of unconventional and ultra-tight media including some geomechanical processes, but are not easily used for scientific investigations of micro-scale processes and phenomena in the vicinity of fractures where important behaviors that may control flow in these media occur [*Moridis and Freeman*, 2014].

Simulators useful for both scientific or commercial purposes have also been developed [*Moridis and Freeman*, 2014]. Freeman et al. (2011) discuss the impacts of Knudsen diffusion, molecular diffusion, and liquid diffusion to gas transport. Because surface diffusion and configurational diffusion are poorly described and few if any measurements have been made to investigate these processes in any heterogeneous medium particularly under multiple phase, multiple component conditions found in the earth's subsurface, these were not included in the model. These authors conclude that the advection-diffusion model adequately describes behavior for permeabilities greater than $10^{-12}m^2$, but lower permeabilities require the use of the Dusty Gas Model [*Thorstenson and Pollock*, 1989b]. They further suggest a permeability estimation method based on the Dusty Gas system of equations with a multi-component gas, using the compositional deviation from theoretical composition to refine the permeability estimate.

Moridis and Freeman (2014) discuss two modules written for the TOUGH+ code to enable modeling of a mixture of gases and water through natural media containing nanoporous regions including shales and tight sandstones. Codes like this approach behavior on the grid-block scale, and assume that material properties are uniform across the grid block. The scales of the grid blocks are determined by the modeler based on available data and computational needs. Because the modules function with the TOUGH+ code, they include functionality of this code including the physics and thermodynamics of mass and heat flow through porous media, and account for most known processes [*Moridis and Freeman*, 2014]. This includes gas sorption on minerals and kerogen, Knudsen diffusion through incorporation of the Klinkenberg parameter and the Dusty Gas Model. Two methods are included to handle porosity change with pressure, and the modules include gas solubility into the aqueous phase. The nomenclature table lists 87 terms (not including those with multiple subscripts and superscripts). Use of the code to evaluate a model of an experiment or reservoir will likely require parameterization along the same order of magnitude requiring data describing behavior and reasonable estimation techniques based on solid

science. Currently, there are few efforts to link pore-scale observations to grid-block scale parameters, with modelers using pore-scale observations to support their conceptual models.

In describing a code to evaluate gas flow through hydraulically fractured shale, Civan (2013) presents a nice table broadly naming many processes of interest. For each, a constitutive model and set of parameters are required. Codes like these that account for numerous processes are very important because they allow investigation of the relative importance of each process based on the individual process models they are based on. Parameterizing models for evaluation using these codes, and understanding the constitutive models they are composed from is critically important in effectively using the codes scientifically or commercially.

Akkutlu and Fathi (2012) model gas transport in organic-rich shales with a matrix having dual-porosity continua associated with organic and inorganic pores, and a fracture continuum. In their model, gas in kerogen is transported through small pores or along surfaces to larger pores in the mineral matrix, where viscous flow transports the gas to larger fractures. In the model, the kerogen is distributed throughout the matrix. They suggest that gas transport in mineral pores can be modeled as Darcy flow (no-slip), but transport in pores in kerogen by slip flow. The Darcy flow is stress dependent, attributed to slit-shaped pores. They validate their model on core-plug permeability measurements, and then use the model to investigate the impact of the nonuniform distribution of kerogen, showing that molecular processes and the distribution of kerogen are important to gas transport. Measurements are required to quantify both.

Two models that have been shown to adequately describe reservoir behavior are worth mentioning. Silin and Kneafsey (2012) created an analytical model of a bounded-stimulated-domain of a horizontal well within fractured shale that accounts for both compression and adsorption gas storage. Using the method of integral relations, they obtain an analytical formula approximating the solution to the nonlinear pressure diffusion equation. Their model defines a decline curve, predicting two stages of production. At early times, the production rate declines with the reciprocal of the square root of time, however at later times, the rate declines exponentially. The model has been compared to and verified by successfully matching monthly production data from a number of shale-gas wells collected over several years of operation. Their model considers relatively few factors that may affect gas recovery and incorporates a number of simplifying assumptions, yet matches well data and predicts future performance based on past. In spite of that, it is only a basic step toward understanding shale-gas-recovery mechanisms.

Montiero et al., (2013) propose a model based on continuum flow through the matrix, and gas production from kerogen regions within the shale. In this

model, gas flow is hindered by the boundary at the outer regions of the kerogen, and this layer's properties change over time as gas is produced. This model is mathematically well-informed, but not strongly supported by numerous studies of the pore space in kerogen e.g. [*Ambrose et al.*, 2010; *Chi et al.*, 2015; *Curtis et al.*, 2011; *Desbois et al.*, 2009; *Dewers et al.*, 2012; *Silin and Kneafsey*, 2012; *Sisk et al.*, 2010], however these studies did not probe kerogen porosity at all scales. This model fits declines in gas production rates very well, and points to another physical mechanism that requires further study.

Concluding Remarks
Flow in natural media with nanoporous regions is very complicated, and the number of processes that govern it is large. Numerical codes to integrate and evaluate the ensemble of these processes at the aggregate scale are well-developed. Significant work has been done to understand individual processes governing flow in natural media with nanoporous regions, and tools over the entire range from very simple to very elaborate have been used to assess and understand the pore spaces in these media. The complications, however, of fluid(s) flow in rock with multiscale heterogeneities and anisotropies, particularly in the presence of multiple phases and large gradients are enormous. Better understanding is still required including:
- mechanisms of gas flow in kerogen, including the changes in properties of the kerogen as hydrocarbons are produced or as CO_2 is introduced, to reduce the speculative nature of transport mechanisms [*Florence et al.*, 2007; *Montiero et al.*, 2013; *Wang and Reed*, 2009]
- the interconnection of porous inclusions (typically organic-where gas is thought to primarily be stored) and transport properties (permeability, wettability), and quantify the transport pathways for the produced or introduced fluids [*Akkutlu and Fathi*, 2012; *Ambrose et al.*, 2010]
- processes and their magnitudes under different thermodynamic conditions (pressure, temperature, chemistry, saturations, and pore size) to optimize the desired outcome, for example the relative permeability at the grid block, core, bedding layer, near-fracture environment, and nanoporous matrix grain scales
- importance of processes such as surface diffusion, configurational diffusion, and liquid diffusion to gas and liquid transport [*Freeman et al.*, 2011]

Because of the importance of shale, gaining these additional understandings is important and worthwhile. Scaling up and interpreting nanoscale observations for use in macroscale modeling will be challenging, and efforts that are under way to do this should be continued and enhanced.

References

Akkutlu, I. Y., and E. Fathi (2012), Multiscale Gas Transport in Shales With Local Kerogen Heterogeneities, *SPE Journal*, *2012*(December), 10, doi:10.2118/146422-PA.

Alnoaimi, K. R., C. Duchateau, and A. R. Kovscek (2015), Characterization and Measurement of Multiscale Gas Transport in Shale-Core Samples, *SPE Journal*, doi:10.2118/2014-1920820-PA.

Ambrose, R. J., R. C. Hartman, M. Diaz Campos, I. Y. Akkutlu, and C. Sondergeld (2010), New Pore-scale Considerations for Shale Gas in Place Calculations, in *SPE Unconventional Gas Conference* edited, Society of Petroleum Engineers, Pittsburgh, Pennsylvania, USA, doi:10.2118/131772-MS.

Anderson, W. (1986), Wettability Literature Survey- Part 2: Wettability Measurement, *Journal of Petroleum Technology*(November), 17, doi:10.2118/13933-PA.

Arthur, M. A., and D. R. Cole (2014), Unconventional Hydrocarbon Resources: Prospects and Problems, *Elements*, *10*(4), 257-264, doi:http://elements.geoscienceworld.org/content/10/4/257.abstract.

Bachu, S., and B. Bennion (2008), Effects of in-situ conditions on relative permeability characteristics of CO2-brine systems, *Environmental Geology*, *54*(8), 1707-1722, doi:10.1007/s00254-007-0946-9.

Barrett, E. P., L. G. Joyner, and P. P. Halenda (1951), The Determination of Pore Volume and Area Distributions in Porous Substances. I. Computations from Nitrogen Isotherms, *Journal of the American Chemical Society*, *73*(1), 373-380, doi:10.1021/ja01145a126.

Bennion, B., and S. Bachu (2005), Relative Permeability Characteristics for Supercritical CO2 Displacing Water in a Variety of Potential Sequestration Zones, in *2005 SPE Annual Technical Conference and Exhibition* edited, Society of Petroleum Engineers, Dallas, Texas, U.S.A., doi:10.2118/95547-MS.

Bennion, B., and S. Bachu (2008), Drainage and Imbibition Relative Permeability Relationships for Supercritical CO2/Brine and H2S/Brine Systems in Intergranular Sandstone, Carbonate, Shale, and Anhydrite Rocks, *SPE Reservoir Evaluation & Engineering*(June), 10, doi:10.2118/99326-PA.

Bennion, D. B. (2002), An Overview of Formation Damage Mechanisms Causing a Reduction in the Productivity and Injectivity of Oil and Gas Producing Formations, *Journal of Canadian Petroleum Technology*, *41*(11), 8, doi:10.2118/02-11-DAS.

Bennion, D. B., and S. Bachu (2007), Permeability and Relative Permeability Measurements at Reservoir Conditions for CO2-Water Systems in Ultra Low Permeability Confining Caprocks, in *SPE Europec/EAGE Annual Conference and Exhibition*, edited, Society of Petroleum Engineers, London, United Kingdom, doi:10.2118/106995-MS.

Blasingame, T. A. (2008), The Characteristic Flow Behavior of Low-Permeability Reservoir Systems, in *2008 SPE Unconventional Reservoirs Conference* edited, Society of Petroleum Engineers, Keystone, Colorado, U.S.A., doi:10.2118/114168-MS.

Britannica, E. (2016), Shale, in *Encyclopædia Britannica Online*, edited, Encyclopædia Britannica Inc., doi:<http://www.britannica.com/science/shale>.

Brown, R. J. S., and I. Fatt (1956), Measurements Of Fractional Wettability Of Oil Fields' Rocks By The Nuclear Magnetic Relaxation Method, in *31st Annual Fall Meeting of the Petroleum*

Branch of the American Institute of Mining, Metallurgical, and Petroleum Engineers, edited, Society of Petroleum Engineers, Los Angeles, doi:10.2118/743-G.

Brunauer, S., P. H. Emmett, and E. Teller (1938), Adsorption of Gases in Multimolecular Layers, *Journal of the Americal Chemical Society*, *60*, 309-319.

Bustin, R. M., A. M. M. Bustin, A. Cui, D. Ross, and V. M. Pathi (2008), Impact of Shale Properties on Pore Structure and Storage Characteristics, in *2008 SPE Shale Gas Production Conference* edited, Society of Petroleum Engineers, Fort Worth, Texas, U.S.A., doi:10.2118/119892-MS.

Carey, J. W., Z. Lei, E. Rougier, H. Mori, and H. Viswanathan (2015), Fracture-permeability behavior of shale, *Journal of Unconventional Oil and Gas Resources*, *11*, 27-43, doi:http://dx.doi.org/10.1016/j.juogr.2015.04.003.

Carles, P., P. Egermann, R. Lenormand, and J. Lombard (2007), Low permeability measurements using steady-state and transient methods , SCA2007-07.

Chalmers, G. R., R. M. Bustin, and I. M. Power (2012), Characterization of gas shale pore systems by porosimetry, pycnometry, surface area, and field emission scanning electron microscopy/transmission electron microscopy image analyses: Examples from the Barnett, Woodford, Haynesville, Marcellus, and Doig units, *AAPG Bulletin*, *96*(6), 1099-1119, doi:10.1306/10171111052.

Chen, G., M. E. Chenevert, M. M. Sharma, and M. Yu (2003), A study of wellbore stability in shales including poroelastic, chemical, and thermal effects, *JPSE*, *38*(3–4), 167-176, doi:http://dx.doi.org/10.1016/S0920-4105(03)00030-5.

Chi, L., Z. Heidari, and A. P. Garcia (2015), Investigation of Wettability and Fluid Distribution in Organic-rich Mudrocks using NMR Two-Phase Simulation, in *SPE Annual Technical Conference and Exhibition* edited, Society of Petroleum Engineers, Houston, Texas, USA, doi:10.2118/175077-MS.

Cipolla, C. L., E. P. Lolon, J. C. Erdle, and B. Rubin (2010), Reservoir Modeling in Shale-Gas Reservoirs, *SPE Reservoir Evaluation & Engineering*(August), doi:10.2118/125530-PA.

Cipolla, C. L., N. R. Warpinski, and M. J. Mayerhofer (2008), Hydraulic Fracture Complexity: Diagnosis, Remediation, And Explotation, in *2008 SPE Asia Pacific Oil & Gas Conference and Exhibition* edited, Society of Petroleum Engineers, Perth, Australia, doi:10.2118/115771-MS.

Civan, F. (2013), Modeling Gas Flow Through Hydraulically-Fractured Shale-gas Reservoirs Involving Molecular-to-Inertial Transport Regimes and Threshold-Pressure Gradient, in *SPE Annual Technical Conference and Exhibition* edited, Society of Petroleum Engineers, New Orleans, Louisiana, USA, doi:10.2118/166324-MS.

Clarkson, C. R., N. Solano, R. M. Bustin, A. M. M. Bustin, G. R. L. Chalmers, L. He, Y. B. Melnichenko, A. P. Radliński, and T. P. Blach (2013), Pore structure characterization of North American shale gas reservoirs using USANS/SANS, gas adsorption, and mercury intrusion, *Fuel*, *103*, 606-616, doi:http://dx.doi.org/10.1016/j.fuel.2012.06.119.

Computer Modelling Group, L. (2016), edited, doi:http://www.cmgl.ca/software/gem2015.

Curtis, M. E., R. J. Ambrose, C. H. Sondergeld, and C. S. Rai (2011), Transmission and Scanning Electron Microscopy Investigation of Pore Connectivity of Gas Shales on the

Nanoscale, in *SPE North American Unconventional Gas Conference and Exhibition* edited, Society of Petroleum Engineers, The Woodlands, Texas, USA, doi:10.2118/144391-MS.

Desbois, G., J. L. Urai, and P. A. Kukla (2009), Morphology of the pore space in claystones – evidence from BIB/FIB ion beam sectioning and cryo-SEM observations, *Earth*, *4*(1), 15-22, doi:10.5194/ee-4-15-2009.

Dewers, T. A., J. Heath, R. Ewy, and L. Duranti (2012), Three-dimensional pore networks and transport properties of a shale gas formation determined from focused ion beam serial imaging, *Int. J. of Oil, Gas and Coal Technology*, *5*(2/3), 229 - 248, doi:10.1504/IJOGCT.2012.046322.

Dubinin, M. M. (1989), Fundamentals of the theory of adsorption in micropores of carbon adsorbents: Characteristics of their adsorption properties and microporous structures, *Carbon*, *27*(3), 457-467, doi:http://dx.doi.org/10.1016/0008-6223(89)90078-X.

Elgmati, M. M., H. Zhang, B. Bai, R. E. Flori, and Q. Qu (2011), Submicron-Pore Characterization of Shale Gas Plays, in *SPE North American Unconventional Gas Conference and Exhibition* edited, Society of Petroleum Engineers, The Woodlands, Texas, USA, doi:10.2118/144050-MS.

Fakcharoenphol, P., B. Kurtoglu, H. Kazemi, S. Charoenwongsa, and Y.-S. Wu (2014), The Effect of Osmotic Pressure on Improve Oil Recovery from Fractured Shale Formations, in *SPE Unconventional Resources Conference – USA*, edited, Society of Petroleum Engineers, The Woodlands, Texas, USA, doi:10.2118/168998-MS.

Fisher, L. R., and J. N. Israelachvili (1979), Direct experimental verification of the Kelvin equation for capillary condensation, *Nature*, *277*(5697), 548-549, doi:http://dx.doi.org/10.1038/277548a0.

Florence, F. A., J. Rushing, K. E. Newsham, and T. A. Blasingame (2007), Improved Permeability Prediction Relations for Low Permeability Sands, in *2007 SPE Rocky Mountain Oil & Gas Technology Symposium* edited, Society of Petroleum Engineers, Denver, Colorado, U.S.A., doi:10.2118/107954-MS.

Freeman, C. M., G. J. Moridis, and T. A. Blasingame (2011), A Numerical Study of Microscale Flow Behavior in Tight Gas and Shale Gas Reservoir Systems, *Transport in Porous Media*, *90*(1), 253-268, doi:10.1007/s11242-011-9761-6.

Freifeld, B. M., T. J. Kneafsey, and F. Rack (2006), On-Site Geologic Core Analysis Using a Portable X-ray Computed Tomographic System, in *New Techniques in Sediment Core Analysis*, edited by R. G. Rothwell, pp. 165–178, The Geological Society of London.

Gannaway, G. (2014), NMR Investigation of Pore Structure in Gas Shales, in *SPE international Student Paper Contest at the SPE Annual Technical Conference and Exhibition* edited, Society of Petroleum Engineers, Amsterdam, The Netherlands, doi:10.2118/173474-STU.

Heath, J. E., T. A. Dewers, B. J. O. L. McPherson, M. B. Nemer, and P. G. Kotula (2012), Pore-lining phases and capillary breakthrough pressure of mudstone caprocks: Sealing efficiency of geologic CO2 storage sites, *International Journal of Greenhouse Gas Control*, *11*, 204-220, doi:10.1016/j.ijggc.2012.08.001.

Heath, J. E., T. A. Dewers, B. J. O. L. McPherson, R. Petrusak, T. C. Chidsey, A. J. Rinehart, and P. S. Mozley (2011), Pore networks in continental and marine mudstones: Characteristics and controls on sealing behavior, *Geosphere*, *7*(2), 429-454, doi:10.1130/ges00619.1.

Hu, Y., D. Devegowda, A. Striolo, A. Phan, T. A. Ho, F. Civan, and R. F. Sigal (2014), Microscopic Dynamics of Water and Hydrocarbon in Shale-Kerogen Pores of Potentially Mixed Wettability, *SPE Journal*, 112-124, doi:10.2118/167234-PA.

Javadpour, F., D. Fisher, and M. Unsworth (2007), Nanoscale Gas Flow in Shale Gas Sediments, *Journal of Canadian Petroleum Technology*, doi:10.2118/07-10-06.

Jones, F. O., and W. W. Owens (1980), A Laboratory Study of Low-Permeability Gas Sands, *Journal of Petroleum Technology*, *32*(09), 1631-1640, doi:10.2118/7551-PA.

King, H. E., A. P. R. Eberle, C. C. Walters, C. E. Kliewer, D. Ertas, and C. Huynh (2015), Pore Architecture and Connectivity in Gas Shale, *Energy & Fuels*, *29*(3), 1375-1390, doi:10.1021/ef502402e.

Klinkenberg, L. J. (1941), The Permeability Of Porous Media To Liquids And Gases, in *American Petroleum Institute Conference Paper, Production Practice*, edited, American Petroleum Institute.

Loucks, R. G., R. M. Reed, S.C. Ruppel, and D.M. Jarvie (2009), Morphology, Genesis, and Distribution of Nanometer-Scale Pores in Siliceous Mudstones of the Mississippian Barnett Shale, *Journal of Sedimentary Research*, *79*(12), 848-861.

Meakin, P., and A. M. Tartakovsky (2009), Modeling and simulation of pore-scale multiphase fluid flow and reactive transport in fractured and porous media, *Reviews of Geophysics*, *47*(3), 47, doi:10.1029/2008RG000263.

Mehmani, A., M. Prodanović, and F. Javadpour (2013), Multiscale, Multiphysics Network Modeling of Shale Matrix Gas Flows, *Transport in Porous Media*, *99*(2), 377-390, doi:10.1007/s11242-013-0191-5.

Montiero, P. J. M., C. H. Rycroft, and G. I. Barenblatt (2013), A mathematical model of fluid and gas flow in nanoporous media, *Proceedings of the National Academy of Sciences*, *109*(50), 20309-20313, doi:10.1073/pnas.1219009109.

Moridis, G. J., and C. M. Freeman (2014), The RealGas and RealGasH2O options of the TOUGH+ code for the simulation of coupled fluid and heat flow in tight/shale gas systems, *Computers & Geosciences*, *65*, 56-71, doi:http://dx.doi.org/10.1016/j.cageo.2013.09.010.

Moridis, G. J., and K. Pruess (2014), User's Manual of the TOUGH+ Core Code v1.5: A General-Purpose Simulator of Non-Isothermal Flow and Thansport Through Porous and Fractured Media*Rep. LBNL-6871E*, 214 pp, Lawrence Berkeley National Laboratory, Berkeley CA, USA.

Nelson, P. H. (2009), Pore-throat sizes in sandstones, tight sandstones, and shales, *AAPG Bulletin*, *93*(3), 329-340, doi:DOI:10.1306/10240808059.

Nobakht, M., and C. R. Clarkson (2011), Analysis of Production Data in Shale Gas Reservoirs: Rigorous Corrections for Fluid and Flow Properties, in *SPE Eastern Regional Meeting*, edited, Society of Petroleum Engineers, Columbus, Ohio, USA, doi:10.2118/149404-MS.

Odusina, E. O., C. H. Sondergeld, and C. S. Rai (2011), NMR Study of Shale Wettability, in *Canadian Unconventional Resources Conference* edited, Society of Petroleum Engineers, Calgary, Alberta, Canada, doi:10.2118/147371-MS.

Ozkan, E., R. S. Raghavan, and O. G. Apaydin (2010), Modeling of Fluid Transfer From Shale Matrix to Fracture Network, in *SPE Annual Technical Conference and Exhibition* edited, Society of Petroleum Engineers, Florence, Italy, doi:10.2118/134830-MS.

Rasband, W. S. (2016), ImageJ, edited, U. S. National Institutes of Health, Bethesda, Maryland, USA, doi: http://imagej.nih.gov/ij/.

Ruppert, L. F., R. Sakurovs, T. P. Blach, L. He, Y. B. Melnichenko, D. F. R. Mildner, and L. Alcantar-Lopez (2013), A USANS/SANS Study of the Accessibility of Pores in the Barnett Shale to Methane and Water, *Energy & Fuels*, *27*(2), 772-779, doi:10.1021/ef301859s.

Sakhaee-Pour, A., and S. Bryant (2012), Gas Permeability of Shale, *SPE Reservoir Evaluation & Engineering*, *August 2012* doi:10.2118/146944-PA.

Schlumberger, I. (2016), doi:https://www.software.slb.com/products/eclipse/unconventional.

Sigal, R. F. (2015), Pore-Size Distributions for Organic-Shale-Reservoir Rocks From Nuclear-Magnetic-Resonance Spectra Combined With Adsorption Measurements, *SPE Journal*(August), 7, doi:10.2118/174546-PA.

Silin, D., and T. J. Kneafsey (2012), Gas Shale: From Nanometer-Scale Observations To Well Modeling, *Journal of Canadian Petroleum Technology*, *51*(6), 464-475, doi:10.2118/149489-PA.

Sing, K. S. W. (1985), Reporting Physisorption Data for Gas/Solid Systems with Special Reference to the Determination of Surface Area and Porosity, *Pure Appl. Chem.*, *57*(4), 603-619, doi:10.1351/pac198557040603.

Sisk, C., E. Diaz, J. Walls, A. Grader, and M. Suhrer (2010), 3D Visualization and Classification of Pore Structure and Pore Filling in Gas Shales, in *SPE Annual Technical Conference and Exhibition* edited, Society of Petroleum Engineers, Florence, Italy, doi:10.2118/134582-MS.

Slatt, R., and N. O'Brien (2014), Variations in Shale Pore Types and Their Measurement, in *Unconventional Resources Technology Conference* edited, Denver, Colorado, USA, doi:10.15530/urtec-2014-1921688.

Sondergeld, C. H., R. J. Ambrose, C. S. Rai, and J. Moncrieff (2010), Micro-Structural Studies of Gas Shales, in *SPE Unconventional Gas Conference* edited, Society of Petroleum Engineers, Pittsburgh, Pennsylvania, USA, doi:10.2118/131771-MS.

Thorstenson, D. C., and D. W. Pollock (1989a), Gas Transport in Unsaturated Porous Media: The Adequacy of Fick's Law, *Reviews of Geophysics*, *27*(1), 61-78.

Thorstenson, D. C., and D. W. Pollock (1989b), Gas transport in unsaturated zones: Multicomponent systems and the adequacy of Fick's laws, *Water Resources Research*, *25*(3), 477-507, doi:10.1029/WR025i003p00477.

Tinni, A., E. Odusina, I. Sulucarnain, C. Sondergeld, and C. S. Rai (2015), Nuclear-Magnetic-Resonance Response of Brine, Oil, and Methane in Organic-Rich Shales, *SPE Reservoir Evaluation & Engineering*(August), 7, doi:10.2118/168971-PA.

Tolman, R. C. (1949), The Effect of Droplet Size on Surface Tension, *The Journal of Chemical Physics*, *17*(3), 333-337, doi:doi:http://dx.doi.org/10.1063/1.1747247.

Tomutsa, L., D. Silin, and V. Radmilovic (2007), Analysis of Chalk Petrophysical Properties By Means of Submicron-Scale Pore Imaging and Modeling, *SPE Reservoir Evaluation & Engineering*, *10*(3), 285-293, doi:10.2118/99558-PA.

Trebotich, D., and D. T. Graves (2015), An Adaptive Finite Volume Method for the Incompressible Navier-Stokes Equations in Complex Geometries, *Comm App Math Com Sc*, *10*(1), 43-82, doi:10.2140/camcos.2015.10.43.

Umeda, K., R. Li, Y. Sawa, H. Yamabe, Y. Liang, H. Honda, S. Murata, T. Matsuoka, T. Akai, and S. Takagi (2014), Multiscale Simulations of Fluid Flow in Nanopores for Shale Gas, in *International Petroleum Technology Conference* edited, International Petroleum Technology Conference, Kuala Lumpur, Malaysia, doi:10.2523/17949-MS.

Vega, B., A. Dutta, and A. Kovscek (2014), CT Imaging of Low-Permeability, Dual-Porosity Systems Using High X-ray Contrast Gas, *Transport in Porous Media*, *101*(1), 81-97, doi:10.1007/s11242-013-0232-0.

Wang, F. P., and R. M. Reed (2009), Pore Networks and Fluid Flow in Gas Shales, in *2009 SPE Annual Technical Conference and Exhibition* edited, Society of Petroleum Engineers, New Orleans, Louisiana, USA, doi:10.2118/124253-MS.

Watson, A. T., and J. Mudra (1994), Characterization of Devonian Shales With X-Ray-Computed Tomography, *SPE Form. Eval.*, doi:10.2118/22943-PA.

Webb, S., and K. Pruess (2003), The Use of Fick's Law for Modeling Trace Gas Diffusion in Porous Media, *Transport in Porous Media*, *51*(3), 327-341, doi:10.1023/A:1022379016613.

White, F. M. (1979), *Fluid Mechanics*, 701 pp., McGraw-Hill Book Company.

Wu, Y.-S. (2015), *Multiphase Fluid Flow in Porous and Fractured Reservoirs*, Gulf Professional Publishing.

Wu, Y.-S., K. Pruess, and P. Persoff (1998), Gas Flow in Porous Media With Klinkenberg Effects, *Transport in Porous Media*, *32*(1), 117-137, doi:10.1023/A:1006535211684.

Yoon, H., and T. A. Dewers (2013), Nanopore structures, statistically representative elementary volumes, and transport properties of chalk, *Geophysical Research Letters*, *40*(16), 4294-4298, doi:10.1002/grl.50803.

Zhang, P., L. Hu, J. N. Meegoda, and S. Gao (2015), Micro/Nano-pore Network Analysis of Gas Flow in Shale Matrix, *Scientific Reports*, *5*, 13501, doi:10.1038/srep13501.